Effect of precession with arbitrary frequency on local stability of rotating flow

Me Me Naing and Y Fukumoto

Department of Mathematics, Yangon University, Kamayut 11041, Yangon Division, Myanmar, email: memenaing04@gmail.com

Faculty of Mathematics and Mathematical Research Center for Industrial Technology, Kyushu University, 744 Motooka, Nishi-ku, Fukuoka, 819-0395, Japan

1. Abstract

We revisit the local stability, to three-dimensional disturbances, of rotating flows with circular streamlines, whose rotation axis executes constant precessional motion about an axis perpendicular to itself. In the rotating frame, the basic flow is steady velocity field linear in coordinates in an unbounded domain constructed by Kerswell (1993), and admits the use of the WKB method. For small precession frequency, we recover Kerswell's result. A novel instability is found at large frequency for which the axial wavenumber executes an oscillation around zero; drastic growth of disturbance amplitude occurs only in an extremely short time interval around the time where the axial wavenumber vanishes. In the limit of infinite precession frequency, the growth rate exhibits singular behavior with respect to a parameter characterizing the tilting angle of the wave vector.

2. Formulation and WKB characteristic equations

Let us consider a precessing rotating flow, of infinite expanse, whose velocity field is linear in coordinates, with angular velocity equal to unity, and whose rotating axis itself is rotated about an axis perpendicular to itself, with angular frequency ϵ. Otherwise stated, we are concerned with local stability of a rotating flow subjected to an external Coriolis force.

We choose, as the basic state relative to the rotating frame,

$$\boldsymbol{U}(x,y,z) = (-y, x - 2\epsilon z, 0), \tag{1}$$

the same one analyzed by Kerswell (1993). The flow is rotating about the z-axis which is itself rotating at constant angular velocity ϵ about the x-axis. The precessional angular velocity is written vectorially as $\boldsymbol{\Omega} = (\epsilon, 0, 0)$. If the boundaries are ignored, the basic flow is an exact solution of the Euler and even of the Navier-Stokes equations, augmented by the Coriolis force, notably for an arbitrary value of ϵ. We pose no restriction on ϵ. Calculation is made of the growth rate of three-dimensional disturbances of infinitesimal amplitude for both small and large values of precession frequency $|\epsilon|$. The emphasis is put on a demonstration of instability for large values $|\epsilon|$, the other extreme from Kerswell's treatment (1993). We assume that the fluid is inviscid and incompressible.

The analysis is made in the rotating frame in which the basic rotating axis is maintained at the z-axis. The pressure varies along the z axis as $p = (x^2 + y^2)/2 + 2\epsilon z^2 - 2\epsilon xz$. Incidentally Mahalov (1993) considered the basic flow $\boldsymbol{U}_{\mathrm{Ma}}(x,y,z) = (-y, x, -2\epsilon y)$ for a precessing rotating flow with the same precessional angular velocity $\boldsymbol{\Omega} = (\epsilon, 0, 0)$. The boundary condition and the imposed far field pressure would select a realizable local field. The local stability of Mahalov's flow was investigated in our previous investigation (Me Me Naing and Fukumoto 2009).

The disturbance is governed by the Euler equations augmented by the Coriolis force. In harmony with the linear dependence, in coordinates, of the velocity profile of the basic flow, we may superimpose the following form of three-dimensional localized disturbance velocity $\boldsymbol{u}'$ and pressure p'

$$[\boldsymbol{u}'(\boldsymbol{x},t), p'(\boldsymbol{x},t)] = \exp(\mathrm{i}\boldsymbol{k}(t)\cdot\boldsymbol{x})[\boldsymbol{a}(t), \tilde{p}(t)], \tag{2}$$

on the basic flow, where $\boldsymbol{k}(t)$ is the time dependent wave vector (Bayly 1986). We are concerned with amplification or non-amplification of the amplitude $\boldsymbol{a}(t)$ and $\tilde{p}(t)$. These are substituted into the Euler equations and terms quadratic in disturbance amplitude are discarded. Then the linearized Euler equations are reduced to a coupled system of ordinary differential equations:

$$\frac{\mathrm{d}\boldsymbol{k}}{\mathrm{d}t} = -\mathcal{D}^T\boldsymbol{k}, \tag{3}$$

$$\frac{\mathrm{d}\boldsymbol{a}}{\mathrm{d}t} = \left(\frac{2\boldsymbol{k}\boldsymbol{k}^T}{k^2} - I\right)\mathcal{D}\boldsymbol{a} - 2\left(\boldsymbol{\Omega}\times\boldsymbol{a} - [(\boldsymbol{\Omega}\times\boldsymbol{a})\cdot\boldsymbol{k}]\frac{\boldsymbol{k}}{k^2}\right), \tag{4}$$

together with the incompressibility condition

$$\boldsymbol{k}\cdot\boldsymbol{a} = 0, \tag{5}$$

where $k = |\boldsymbol{k}| = (k_1^2 + k_2^3 + k_3^2)^{1/2}$, $\boldsymbol{I}$ is the 3×3 unit matrix, superscript T stands for taking the transpose, and $\mathcal{D}$ is a 3×3 constant matrix defined by

$$\mathcal{D} = \left[\frac{\partial U_i}{\partial x_j}\right] = \begin{bmatrix} 0 & -1 & 0 \\ 1 & 0 & -2\epsilon \\ 0 & 0 & 0 \end{bmatrix}. \tag{6}$$

With use of an overdot for differentiation in t, equation (3) is written in component wise as $(\dot{k_1}, \dot{k_2}, \dot{k_3}) = (-k_2, k_1, 2\epsilon k_2)$ and equation (4) is written explicitly as follows:

$$\begin{bmatrix} \dot{a_1} \\ \dot{a_2} \\ \dot{a_3} \end{bmatrix} = \frac{1}{k^2} \begin{bmatrix} A_{11} & A_{12} & A_{13} \\ A_{21} & A_{22} & A_{23} \\ A_{31} & A_{32} & A_{33} \end{bmatrix} \begin{bmatrix} a_1 \\ a_2 \\ a_3 \end{bmatrix}, \tag{7}$$

where

$$A_{11} = 2k_1k_2, A_{12} = -{k_1}^2 + {k_2}^2 + {k_3}^2 + 2\epsilon k_1k_3, A_{13} = -6\epsilon k_1k_2,$$
$$A_{21} = -{k_1}^2 + {k_2}^2 - {k_3}^2, A_{22} = -2k_1k_2 + 2\epsilon k_2k_3, A_{23} = 4\epsilon {k_1}^2 - 2\epsilon {k_2}^2 + 4\epsilon {k_3}^2,$$
$$A_{31} = 2k_2k_3, A_{32} = -2k_1k_3 - 2\epsilon({k_1}^2 + {k_2}^2), A_{33} = -6\epsilon k_2k_3.$$

Equation (3) has the following general solution:

$$\boldsymbol{k} = (\sin\theta\cos t, \sin\theta\sin t, \cos\theta - 2\epsilon\sin\theta\cos t), \tag{8}$$

where θ is a constant close, if $|\epsilon| \ll 1$, to the inclination angle of the wave vector $\boldsymbol{k}$ from the rotation (z-) axis. With this form, (4) serves as a matrix Floquet problem.

3. Influence of weak precession

This section is concerned with a concise description of the case of a weak external Coriolis force. For handling these characteristic equations, it may be expedient to employ variables introduced by Bayly *et al.* (1996) that reduce the three-component system (4) to a two-component system of periodic coefficients with period 2π. We decompose vectors into components in the xy-plane denoted by subscript $\perp$ and the scalar component parallel to the z-axis and write

$$\boldsymbol{U} = \begin{bmatrix} \boldsymbol{U}_\perp \\ -2\epsilon y \end{bmatrix}, \qquad \mathcal{D} = \begin{bmatrix} \mathcal{D}_\perp & \begin{matrix} 0 \\ -2\epsilon \end{matrix} \\ \begin{matrix} 0 & 0 \end{matrix} & 0 \end{bmatrix}. \tag{9}$$

This decomposition manifests a salient feature of the problem by rewriting (3) into

$$\mathrm{d}\boldsymbol{k}_\perp/\mathrm{d}t = -\mathcal{D}_\perp^T\boldsymbol{k}_\perp + 2\epsilon k_2, \quad \mathrm{d}k_3/\mathrm{d}t = 2\epsilon\sin\theta\sin t. \tag{10}$$

The perpendicular component $\boldsymbol{k}_\perp$ of $\boldsymbol{k}$ decouples from the parallel component. Peculiar to the basic field (9), the z-component k_3 varies with time t, unlike the cases so far investigated. This fact turns out to be responsible for an unusual behavior of the growing mode at large values of $|\epsilon|$.

We introduce the amplitude of the disturbance vorticity

$$\boldsymbol{b} = \boldsymbol{k} \times \boldsymbol{a}, \tag{11}$$

and new variables

$$p = \frac{k}{k_\perp} \boldsymbol{k}_\perp \cdot \boldsymbol{a}_\perp, \quad q = \frac{k}{k_\perp} b_3, \tag{12}$$

where use has been made of $k_\perp = |\boldsymbol{k}_\perp|$ (Bayly *et al.* 1996). As a consequence, (3) and (4) are reduced to

$$\frac{\mathrm{d}}{\mathrm{d}t} \begin{bmatrix} p \\ q \end{bmatrix} = \begin{bmatrix} L_{11} & L_{12} \\ L_{21} & L_{22} \end{bmatrix} \begin{bmatrix} p \\ q \end{bmatrix}, \tag{13}$$

where the matrix entries are

$$\begin{aligned} L_{11} &= \frac{\mathrm{d}}{\mathrm{d}t} \log \frac{k_\perp}{k} - \frac{4\epsilon k_2 k_3}{k_\perp^2} + \frac{2k_3 \dot{k}_3}{k_\perp^2} + \frac{\dot{k}_3}{k_3}, \\ L_{12} &= \frac{2k_3^2}{k^2 k_\perp^2} \boldsymbol{k}_\perp^T \mathcal{H} \boldsymbol{k}_\perp + \frac{2\epsilon k_1 k_3}{k^2}, \\ L_{21} &= -\frac{1}{k_3}(2k_3 + 4\epsilon k_1), \quad L_{22} = -\frac{\mathrm{d}}{\mathrm{d}t} \log \frac{k_\perp}{k}, \end{aligned} \tag{14}$$

supplemented by

$$\mathcal{H} = \mathcal{D}_\perp \begin{bmatrix} 0 & 1 \\ -1 & 0 \end{bmatrix}.$$

The detail of calculation may be referred to Bayly *et al.* (1996) and Lifschitz (1994).

For very small values of $|\epsilon|$, when expanded in powers of ϵ, (13) is approximated by the Mathieu equation:

$$\ddot{q} + (u + 2\epsilon a_1 \cos t) q = 0, \tag{15}$$

where

$$u(\theta) = 4\cos^2\theta, \qquad a_1(\theta) = -3\cos\theta\sin\theta + 8\cos^3\theta\sin\theta.$$

Repeating the procedure of using the Mathieu method (Ince 1956), the same one as for Mahalov's flow (Me Me Naing and Fukumoto 2009), we find that the parametric resonance instability occurs around $u = 1/4, 1/2$ and $9/4$ or around $\theta = \pm\cos^{-1}(1/4), \pm\cos^{-1}(1/2)$ and $\pm\cos^{-1}(3/4)$. The primary mode is the subharmonic instability occurring around $\theta = \pm\cos^{-1}(1/4)$ with $\sigma \approx 5\sqrt{15}|\epsilon|(1 - 75\epsilon^2/64)/32$.

Thus Kerswell's result (1993) is restored to $O(\epsilon)$ by our asymptotic analysis. Kerswell's flow shares the same growth-rate value, to $O(|\epsilon|)$, with Mahalov's flow. Note that the reduced system of equations (13) are not suited for numerical computation over a wide range of θ, because the coefficients (15) become singular when k_3 passes through zero for θ close to $\pi/2$. This is more liable to occur for larger values of ϵ as will be explored subsequently.

4. Influence of strong precession

As is read off from (8), the magnitude $k_\perp = |\sin\theta|$ of the horizontal wave vector never vanishes unless $\theta = 0$. But the axial wavenumber k_3 passes through zero at the time t^*

when $\cos\theta - 2\epsilon\sin\theta\cos t^* = 0$ is fulfilled. Given θ $(0 \leq \theta \leq \pi)$, this occurs twice per period if $\epsilon > \cot\theta/2$. Given ϵ of whatever small value in magnitude, $k_3 = 0$ occurs for $\theta_c < \theta \leq \pi/2$ with θ_c defined by $\cot\theta_c = 2\epsilon$. The method of reducing the variables to p and q gets into trouble when k_3 crosses zero at some instant, in the sense that equation (12) is not invertible for $\boldsymbol{a}$ and b. For large value of $|\epsilon|$, $k_3 = 0$ necessarily occurs and use of the reduced amplitude equation (13) is forbidden, as suggested by divergence of L_{11} and L_{21}. We have no way but to appeal to the original amplitude equation (7), supplemented by (8).

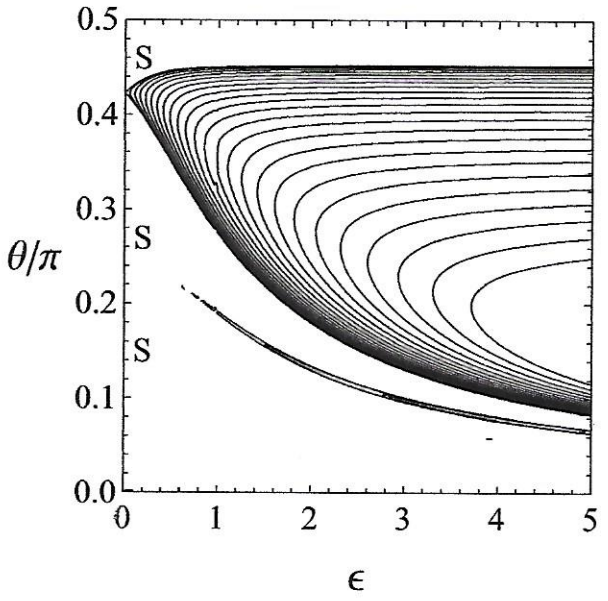

Figure 1. Contours of the growth rate, in the (ϵ, θ) plane, calculated from (7) for a wider range of ϵ $(0 \leq \epsilon \leq 5)$. The stability region is marked with S. For given ϵ, the maximum growth rate is attained at the inclination angle θ shown by the dashed line. The boundary curves correspond to $\sigma = 0$. The increment of σ between neighboring contours is $\Delta\sigma = 0.2/2\pi$.

Figure 1 shows the growth-rate contours calculated from (7) over a wider range of ϵ $(0 \leq \epsilon \leq 5)$. At $\epsilon = 0$, the instability band emanates from $\theta = \cos^{-1}(1/4)$ $(\theta/\pi \approx 0.419569)$. As $|\epsilon|$ is increased, the band becomes wider with the maximum growth rate larger which is attained at a smaller angle θ. Given ϵ, the maximum value of the Floquet exponent is drawn up to as large as $\epsilon = 1000$, in figure 2. The angle θ at which the maximum exponent is attained is simultaneously included with a dashed line. We observe from figure 2 that the maximum growth rate increases monotonically with ϵ. Conceivably, the graph indicates a tendency of saturation of the growth rate, though, at this stage, it is hard to conclude whether σ tends to a finite value or not in the limit of $|\epsilon| \to \infty$.

To have an idea of the manner in which the amplification of the disturbance amplitude is caused, we display, in figure 3, the x-component, $a_1(t)(0 \leq t \leq 2\pi)$, of the numerical solution for $\epsilon = 100$ and $\theta = 0.011983\pi$ of the most unstable mode, with

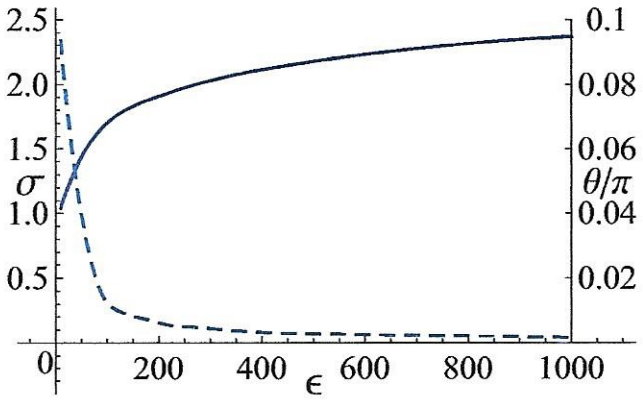

Figure 2. The maximum growth rate σ, along with inclination angle θ, as functions of ϵ, calculated from (7).

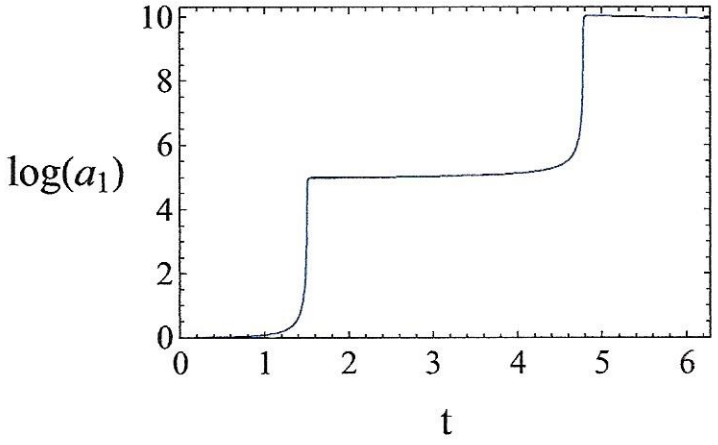

Figure 3. The x component of the solution of (7) for $\epsilon = 100$ and $\theta = 0.011983\pi$. During in a short time interval $a_1(t)$ growth rapidly.

the vertical axis in log-scale. It is seen from figure 3 that the amplitude grows drastically during a very short time around t^* at which $k_3 = \cos\theta - 2\epsilon \sin\theta \cos t^* = 0$. This occurs twice in each period, at $t^* \approx 1.59493$ and 4.77601, being consistent with figure 3. As is clearly seen from figure 3, the amplitude grows gradually in almost the whole period except for these short time interval around t^*. In order to answer the question of whether the growth rate is finite or not, it may suffice to estimate the solution, during the short time range centered on $t = t^*$. We will make an attempt to estimate the growth rate, with the aid of a local analysis in time.

Consider the amplitude equations for the time range divided into two parts: the almost whole range except for short time intervals around t^*. Although the largest growth rate occurs at $|\theta| \ll 1$ for $|\epsilon| \gg 1$, the situation is rather subtle when t comes close to t^*. During the extremely short time around $t = t^*$, of duration about $1/(|\epsilon| \sin t^*)$, as will subsequently be explained, $|k_3|$ becomes comparable with $|\theta|$ or even smaller than

$|\theta|$ and therefore we must keep the terms proportional to $\sin^2\theta, k_1k_2$, k_1^2 and k_2^2 say, in the amplitude equation (7). By taking $\sin\theta \to \theta$ for the short moments around t^*, the wave vector (8) simplifies to

$$\boldsymbol{k} \approx (\theta\cos t, \theta\sin t, 1-2\epsilon\theta\cos t)\,. \tag{16}$$

The amplitude equation (7) then gives way, in the limit of $\cos\theta \to 1$ and $\sin\theta \to 0$, to

$$\begin{bmatrix} \dot{a_1} \\ \dot{a_2} \\ \dot{a_3} \end{bmatrix} \approx \frac{\epsilon\theta^2}{\theta^2+k_3^2} \begin{bmatrix} 0 & 0 & -6\cos t^*\sin t^* \\ 0 & 0 & 4\cos^2 t^* - 2\sin^2 t^* \\ 0 & -2 & 0 \end{bmatrix} \begin{bmatrix} a_1 \\ a_2 \\ a_3 \end{bmatrix}. \tag{17}$$

We keep in mind from the definition that $k_3 = 1-2\epsilon\theta\cos t^* \approx 0$ or $\cos t^* \approx 1/(2\epsilon\theta)$.

We can make a crude estimate, on the ground of (17), of how the velocity amplitude $\boldsymbol{a}(t)$ is amplified during the short time interval around $t = t^*$. Define the local time τ around t^* by $t = t^* + \tau$. Then $k_3 = 1-2\epsilon\theta\cos(t^*+\tau)$ is expanded in a power series in τ as

$$k_3 = 1-2\epsilon\theta\cos(t^*+\tau) = 2\epsilon\theta\sin t^*\tau + \frac{1}{2}\tau^2 + \mathrm{O}(\tau^3). \tag{18}$$

From $\epsilon\theta\cos t^* = 1/2$, $|\sin t^*| = \sqrt{1-1/(4\epsilon^2\theta^2)}$. The integration range is $t^*-\delta t < t^*+\tau < t^*+\delta t$, or $-\delta t < \tau < \delta t$, for a short but sufficiently long time interval $2\delta t$ for the drastic amplification process to be completed. Once the largest eigenvalue $\lambda(t)$ is found, the velocity amplitude is estimated from above as $|\boldsymbol{a}(\mathrm{t})| \le \mathrm{e}^{\int_{-\delta t}^{\delta t}\lambda \mathrm{d}\tau}\,|\boldsymbol{a}(0)|$. This rapid amplification takes place at the two short intervals around t^* during one period $T = 2\pi$. To translate this short-time interval analysis into the Floquet exponent σ, we merely put

$$\sigma = 2\int_{-\delta t}^{\delta t} \lambda \mathrm{d}\tau/T, \tag{19}$$

where λ is the largest eigenvalue.

In view of equation (17) for $|k_3| \ll \theta$ in the immediate neighborhood of $t = t^*$, the eigenvalue $\lambda(t)$ could be of the same order as

$$\lambda \approx \frac{2|\epsilon|\theta^2}{\theta^2+k_3^2}, \tag{20}$$

because $|\sin t^*| \approx 1$ and $|\cos t^*|$ is very small. We retain, in (18), $k_3 \approx 2\epsilon\theta\sin t^*\tau$ to first order in τ for $|\tau| \ll 1$, and evaluate the integral $\int_{-\delta t}^{\delta t}\lambda \mathrm{d}t$ in the following way,

$$\int_{-\delta t}^{\delta t} \lambda \mathrm{d}\tau \approx \frac{1}{2|\epsilon|\sin^2 t^*} \int_{-\delta t}^{\delta t} \frac{\mathrm{d}\tau}{\tau^2 + \frac{1}{4\epsilon^2\sin^2 t^*}} \approx \frac{\pi}{\sin t^*}, \tag{21}$$

for $\delta t \gg 1/(2|\epsilon|\sin t^*)$. Note that δt may be very small value for $|\epsilon| \gg 1$. As $\sin t^*$ is close to 1, we speculate that the Floquet exponent could be finite in the limit of $|\epsilon| \to \infty$.

For a large value $\epsilon = 100$ for example, $\theta \approx 0.011916\pi$ for the maximum growth rate as is seen from figure 2. Thus $\epsilon\theta \approx 3.74352$, and we may take

$$\int_{-\delta t}^{\delta t} \lambda \mathrm{d}\tau \approx \pi, \quad e^{\int_{-\delta t}^{\delta t}\lambda \mathrm{d}\tau} \approx e^{\pi} \approx 23.1407, \tag{22}$$

which is not very different from the numerical solution (figure 3). The contribution from the two moments t^* to the Floquet exponent is

$$2\int_{t^*-\delta t}^{t^*+\delta t} \lambda \mathrm{d}t/T \approx 1. \tag{23}$$

This value accounts for a substantial part of the growth rate $\sigma = 1.70144$ for $\epsilon = 100$ (see figure 2).

5. Conclusion

Recently, global stability analyses have been developed to seek different instability mechanisms (Fukumoto and Hattori 2005, Zhang and Liao 2009, Zhang *et al.* 2010), and have been extended to weakly nonlinear regime for the elliptical instability (Mason and Kerswell 1999, Sipp 2000, Rodrigues and Luca 2009, Mie and Fukumoto 2010) and for the precessional instability with no strain (Mason and Kerswell 2002, Meunier *et al.* 2008, Lehner *et al.* 2010). The nonlinear interaction of disturbances, the modification of mean flow by the nonlinear and the boundary layer effects, and the viscous dissipation may significantly alter the evolution of linearly excited waves (*e.g.* Mason and Kerswell 1999, Zhang *et al.* 2010, Fukumoto *et al.* 2010). The nonlinear excitation of waves via the secondary and the tertiary instability brings in chaotic behavior of rotating flows and in transition to turbulence (Mason and Kerswell 1999, Mason and Kerswell 2002, Fukumoto *et al.* 2005). This paper suggests a rich behavior of unstable waves on a precessing rotating flow of arbitrary precession frequency, but the knowledge has been limited to the linear, in amplitude, regime. The nonlinear stage of evolution of excited waves calls for an individual investigation.

References

Bayly B J 1986 Three-dimensional instability of elliptical flow *Phys. Rev. Lett.* **57** 2160-2163

Bayly B J, Holm D D and Lifschitz A 1996 Three-dimensional stability of elliptical vortex columns in external strain flows *Philos. Trans. R. Soc. Lond.* A **354** 895-926

Ince E L 1956 *Ordinary Differential Equations* (Dover Publications, New York) p 384

Kerswell R R 1993 The instability of precessing flow *Geophys. Astrophys. Fluid Dyn.* **72** 107-144

Mahalov A 1993 The instability of rotating fluid columns subjected to a weak external Coriolis force *Phys. Fluids* **5** 891-900

Me Me Naing and Fukumoto Y 2009 Local instability of an elliptical flow subjected to a Coriolis Force *J. Phys. Soc. Japan* **78** 124401